Chapter – 1

Introduction and Literature Survey

CHAPTER 1: Introduction

1.1 Introduction

In recent years, fossil fuels have been crucial for energy generation. However, it will become scarcer in the near future, and research is still being done to find alternative sources that are abundant and recyclable. The world's energy needs are still not fulfilled; as a result, many countries are dependent on developed countries. According to the data published by P. Murphy in the report “IEA Solar Heating & Cooling Programme” in 2015, the global energy consumption rate was approximately 18.5 TW [1]. This global energy need will increase in the coming years due to industrialization in developing and underdeveloped countries and the increasing world population. Based on the current estimations, by 2050, the global annual energy consumption rate will reach 27 TW and almost 50 TW by the end of the century [2]. In the present scenario, the total global energy consumed is ~ 85 % from burning fossil fuels [3]. The future energy needs must be fulfilled using alternative sources to fossil fuels due to their scarcity and environmental impact. Numerous sources indicate the existence of abundant reserves of fossil energy in various forms that are capable of meeting the expected energy demand for several centuries if consumed at the predicted rate [4]. Fossil fuels have undoubtedly been pivotal in propelling humankind forward over the past two centuries.

However, deepening worries about their finite reserves, the ensuing environmental damage, unstable prices, and insecure supply chains have created alternative energy sources with efficient energy conversion technologies. Developing sustainable energy sources, including solar energy, is becoming increasingly essential to meet the world's energy demands. Solar cells, also known as photovoltaic cells, convert solar radiation directly into electrical power. However, efficiently storing this electricity is a big challenge. An electrically storing device is commonly known as a battery. However, batteries continue to hinder technology because of their low energy density and short lifetime [5].

Another promising avenue is converting solar energy, which involves transforming it into hydrogen, which is thought to be an optimal energy carrier for storage and transportation. Considering power consumption, it is estimated that approximately 120,000 TW of solar energy actually reaches the Earth's surface. Because of atmospheric scattering and cloud cover, only 36,000 TW of the energy reaches land, which implies that achieving a photoelectrochemical (PEC) efficiency of only 10% could feasibly fulfill the global energy demand by 2050 [6], [7], [8], [9].

Energy production, conversion, and transformation of hazardous chemical wastes have been feasible using efficient catalysts. Jöns Jakob Berzelius first used the term "catalysis" in 1835. In 1909, Ostwald received the Nobel Prize for his research on reactions that are triggered by the presence of bases and acids. It must be mentioned that the heterogeneous catalysis method developed by Haber for ammonia synthesis has been praised as the most important scientific discovery of the twenty-first century [10]. Heterogeneous catalysis is a highly effective method for generating and converting renewable energy and its carriers.

1.2 Renewable Energy: The Future Solution

Renewable energy sources are natural resources that are inexhaustible and sustainable. It provides a sustainable substitute for fossil fuels, which are depleting and contribute to environmental deterioration, to meet our energy needs while lowering pollution and mitigating climate change. Some renewable energy sources are sunlight, wind, rain, tides, waves, and geothermal heat.

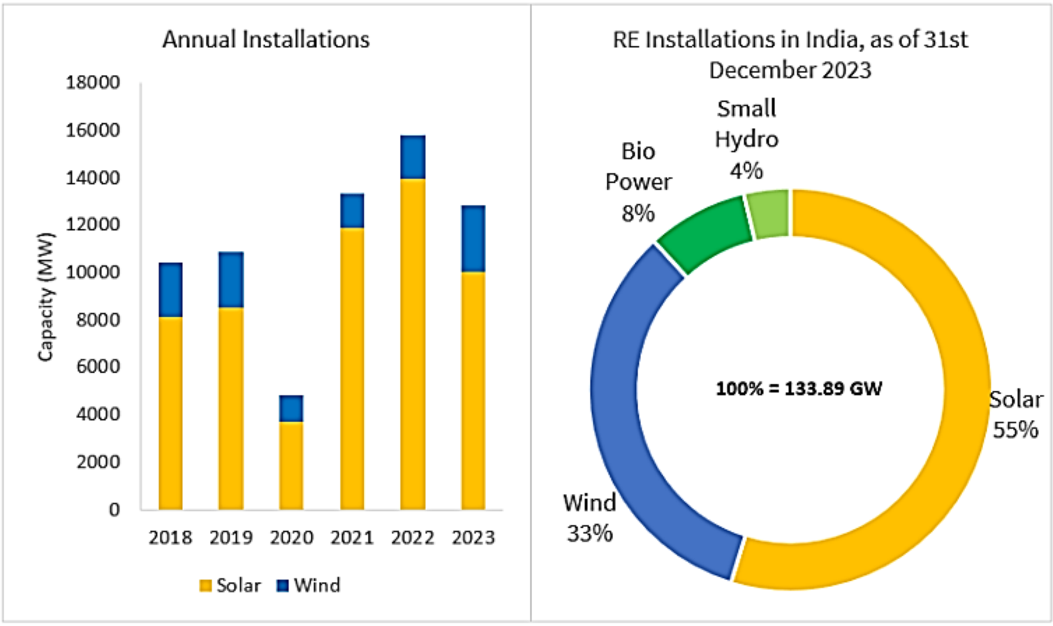

Figure 1.1: Year wise renewable energy installation trends in India (Source: MNRE CEA, JMK research).

1.2.1 Benefits of renewable energy

Environmental Benefits

Since renewable energy sources emit little or no greenhouse gases, they contribute to reducing air pollution and climate change, enhancing public health and the state of the environment.

a) **Energy Security**

Utilizing renewable energy lessens reliance on finite fossil fuels, which are volatile in terms of price and vulnerable to geopolitical unrest. Renewable resources that are readily available locally provide a consistent and varied energy supply, improving energy security.

b) **Economic prospects**

The renewable energy industry offers substantial economic advantages by generating jobs, encouraging innovation, and encouraging investment in regional areas. Furthermore, compared to fossil fuel infrastructure, renewable energy solutions frequently require less maintenance and have lower operational expenses.

c) **Resource Abundance**

It can provide almost an endless supply of clean energy that may be obtained for future generations thanks to the abundance and widespread distribution of renewable energy sources like sunshine, wind, and water.

1.3 Solar energy

Solar energy is generally accessible and abundant. Massive amounts of energy from the Sun can be used practically anywhere on Earth [11]. In contrast to other renewable energy sources that could have restricted geographic reach (such as wind or hydroelectric power), solar energy can be used in urban and rural locations, increasing its accessibility to a broader population. Carbon emissions and air pollution are decreased by solar panel's ability to generate power without releasing greenhouse gases or other pollutants. Since solar panels do not have any moving parts, they are incredibly dependable and long-lasting. Solar panels can last up to 25-30 years with good installation and ongoing upkeep [12]. Solar energy facilitates the decentralization of electricity generation. Individuals and companies can produce electricity and lessen their reliance on centralized power systems by mounting solar panels on roofs or nearby neighborhoods. Energy security is improved by this decentralization, particularly in the event of grid outages or natural calamities. In the long run, solar energy has a ton of innovative and progressive possibilities. Continuous research and development are investigating new materials and technologies to increase the efficiency of solar cells and storage systems. In the long term, solar energy will become even more accessible and efficient due to ongoing innovation.

1.3.1 Solar spectrum

The solar spectrum is the range of wavelengths of electromagnetic energy the Sun generates. The Sun yields a massive amount of energy of ~ 3.471×10^{24} kJ per unit time during the nuclear fusion reaction. Only a tiny portion of ~ 5.0×10^{-11} solar energy makes it to the Earth's surface [11]. As sunlight passes through the atmosphere on its way to the surface, its various wavelengths are affected differently. Understanding the concept of air mass is crucial for interpreting the solar spectrum at different locations and times. The distance sunlight travels through Earth's atmosphere before reaching the surface is known as air mass (AM). It's a method of measuring the amount of atmosphere that sunlight must penetrate. The angle at which sunlight penetrates the atmosphere determines the air mass value; a lower angle corresponds to a higher air mass, and a higher angle (closer to directly overhead) relates to a lower air mass. Figure 1.2 displays the usual solar irradiance spectrum.

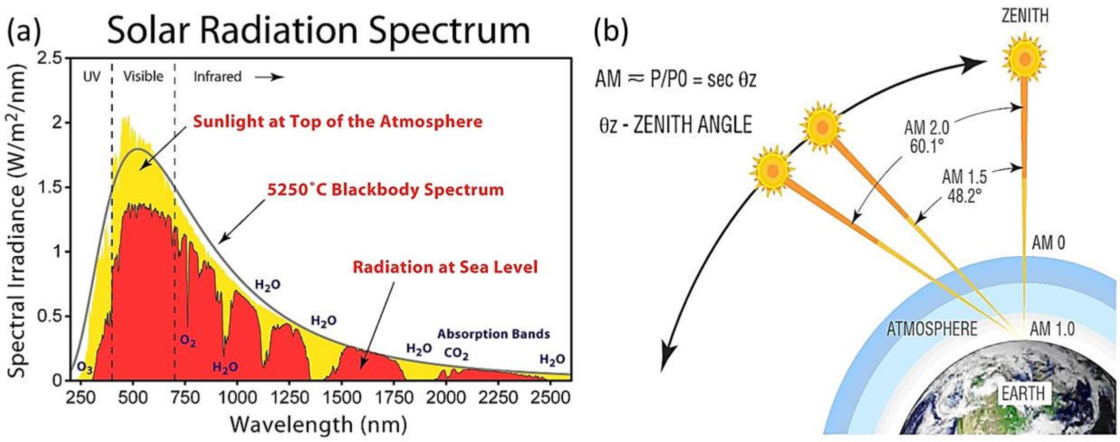

Figure 1.2: (a) Spectral distribution (b) Path length change (in air mass unit) with zenith angle of solar energy [13].

The standard spectrum for space applications is AM 0. It has 1366.1 W/m^2 of integrated power. Two standard spectra are commonly used to define sea-level air mass. The AM 1.5G standard solar spectrum represents the average amount of sunlight received on a flat, horizontal surface and takes into account the Sun's changing angle during the day (the letter "G" stands for "global"). It has 1000 W/m^2 (100 mW/cm^2) of integrated power. The AM 1.5D solar spectrum represents the direct sunlight received on a surface that constantly faces and tracks the Sun's motion (the letter "D" stands for "direct"). It has 900 W/m^2 of integrated power density.

1.3.2 Photoelectrochemical cell

A photoelectrochemical cell (PEC) is a device that uses both photonic and electrochemical processes to convert solar energy into chemical energy [14]. These PECs absorb photons using a semiconductor material, generating electron-hole pairs and then separating and transporting the charge carriers to the semiconductor's surface to participate in redox reactions.

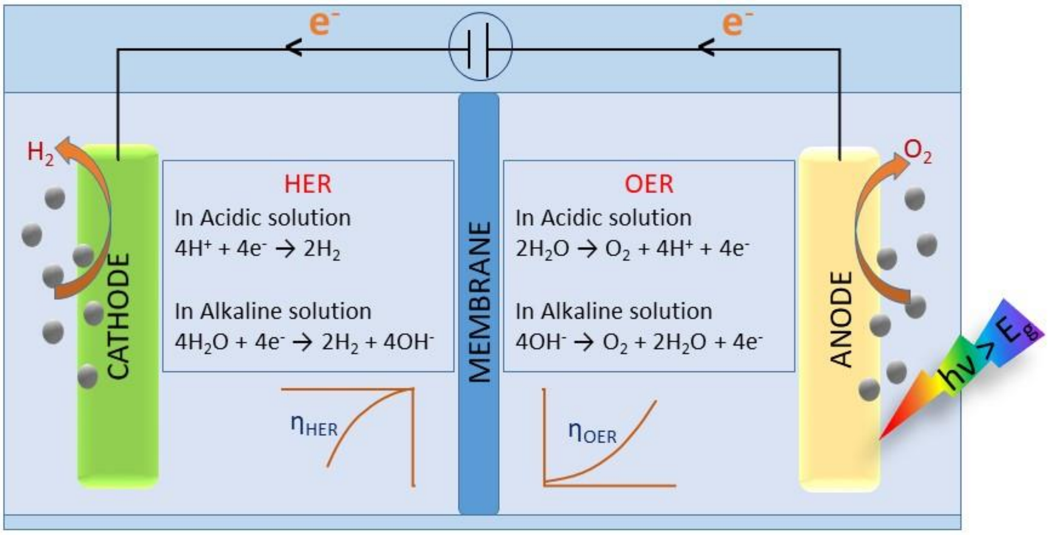

Fig. 1.3: Schematic representation of photoelectrochemical cell.

These cells use energy from the sun to facilitate chemical reactions, primarily by splitting water into hydrogen and oxygen. Hydrogen can be utilized as a clean fuel, demonstrating the potential of PECs for sustainable energy generation.

In 1972, Akira Fujishima and Kenichi Honda discovered the electrochemical photolysis of water splitting using TiO_2 as a catalyst [15]. They suggested that water can be decomposed or split into oxygen and hydrogen under visible light illumination without applying any external voltage. He explained that water electrolysis could occur without the need for external power if any one condition is satisfied: (1) oxygen evolution happens at a potential that is more negative than the HER occurs in usual conditions; (2) HER occurs at a potential more positive than the typical potential for OER; or (3) the potential for OER is made more negative, and the potential for hydrogen evolution is made more positive until the former becomes more negative than the latter.

1.3.3 Components of PEC cells

The function and efficiency of PECs depend on the following essential components:

1) **Photoelectrode**

   The selection of photoelectrode material impacts the absorption of light, separation of charges, and stability. Researchers are exploring advanced materials like nanostructured semiconductors and hybrid composites to improve efficiency.

2) **Counter electrode**

   The counter electrode is responsible for equalizing the electron flow and ensuring effective charge transfer. Using materials with high conductivity and catalytic activity is preferable to reduce energy wastage.

3) **Electrolyte**

The electrolyte facilitates the ionic conduction between the photoelectrode and the counter electrode. A common electrolyte component is a redox couple, such as water, which plays a role in the electrochemical reactions. The selection of the electrolyte can have a substantial effect on the effectiveness and stability of the PEC.

4) **External circuit**

   The external circuit is connected between the counter electrode and photoelectrode or working electrode, ensuring the flow of electrons. The external circuit that joins the photoelectrode and counter electrode enables electron flow. To enhance the PEC's performance, it could incorporate extra parts like resistors, capacitors, or power management programs.

5) **Light source**

   Usually, sunlight supplies the energy needed for the photoelectrode to produce electron-hole pairs. The light source's spectral distribution and intensity influence the PEC's efficiency.

1.4 Hydrogen as a fuel

For over a century, hydrogen has been used on an industrial scale in the Haber-Bosch process to synthesize ammonia, which uses more than 3% of the global hydrogen supply [16]. The need for hydrogen and nitrogen fertilizers is expected to increase due to the necessity to feed the world's growing population. The primary process used nowadays to produce hydrogen on a large scale is steam reforming of natural gas or other hydrocarbons, so lowering greenhouse gas emissions is not as important. Still, hydrogen as an energy carrier is attractive because it is non-toxic, it has the highest calorific value, and burns to generate just water. Hydrogen is transportable, storable, and can be used in mobile modified combustion engines or stationary localized fuel cells [17]. However, there are many obstacles: hydrogen has a poor energy density per volume, is very flammable, and is difficult to store due to its high diffusivity – a phenomenon known as the "Hindenburg dilemma." Hydrogen competes with conventional grid electricity in stationary applications because it has reduced energy losses and doesn't suffer from "boil-off" problems. Although the use of hydrogen in everyday applications is still in its infancy, novel ideas have been put forth and partially developed, such as bicycles driven by hydrogen and portable power banks.

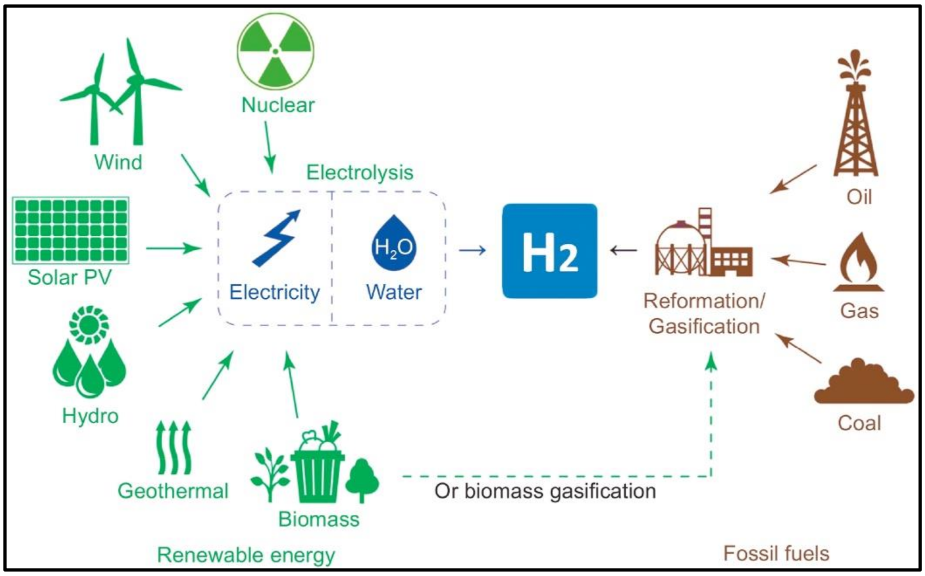

Figure 1.4: Schematic representation of hydrogen production from different energy sources and its application [18].

Fig. 1.4 shows the process of hydrogen production from different sources. Additionally, hydrogen fuel cells show the most significant promise for the transportation industry. Although hydrogen fuel cells are more efficient than internal combustion engines, they have a hefty initial setup cost. Because they don't release CO_2, hydrogen fuel cells also offer a significant advantage over combustion engines. Prominent automakers such as Toyota, BMW, Volkswagen, GM, and Hyundai are investing substantially in developing several types of fuel-cell vehicles. Amazingly, a fuel cell efficiency of only 40% and an electrolyzer efficiency of 70% can result in a grid-to-wheel efficiency of about 30%. By comparison, the efficiency of even the finest internal combustion engines is limited to 28–32% [19]. The car industry has been aiming for increased efficiency since the Industrial Revolution, even though internal combustion engines have had a century's head start. In 1894, Wilhelm Ostwald realized that electrochemistry could help with upcoming worldwide energy problems [20].

Besides its direct application as fuel, hydrogen can be used as a catalyst in the Fischer-Tropsch synthesis and the reverse water-gas shift reaction to create more valuable fuels like methanol, methane, diesel, or gasoline [21]. This method first produces syngas at a high temperature and converts it into usable hydrocarbons. This method can use existing infrastructure to save on storage and transportation expenses. It is possible to reach CO_2 neutrality if it is derived from biogas. Germany established the first industrial plant of this kind, where CO_2 recovered from biogas makes methane and hydrogen produced by electrolysis. The carbon monoxide (CO) created during the process can be used as a feedstock to produce higher hydrocarbons or as a mild specific-impulse fuel. Hydrogen can also be used to hydrogenate biomass, which turns it into a valuable chemical building block. Finding a feasible and clean way to produce hydrogen is still a significant hurdle, as most industrial hydrogen comes from fossil fuels. Hydrogen has an energy content of 119.93 MJ/Kg, up to three times higher than liquid hydrocarbon fuels. One major drawback of hydrogen is that it has a very low density when gaseous and requires much energy to liquefy. Table 1.1 compares the combustion properties of hydrogen with different fuels.

Table 1.1 Comparison of combustion values of different fuels [22].

Fuels	Combustion Value (MJ/Kg)
Hydrogen	119.93
Diesel	42.50
Propane	45.60
Gasoline	44.50
Methane	50.02
Methanol	18.50

1.5 Water splitting

The process of water splitting involves converting liquid water into gaseous oxygen and hydrogen [23][24]. The overall reaction for water splitting is:

$$H_2O\ (l)\ \rightarrow\ H_2(g) + \frac{1}{2}O_2(g)\ \ (\Delta G = 237\ kJ/mol) \qquad (1.1)$$

This reaction is uphill in thermodynamics and is non-spontaneous (Figure 1.5). The energy needed to break apart one water molecule is at least 2.46 eV (ΔG = 237 kJ mol^{-1}) [23]. Since two electrons are involved in this reaction, the standard potential for water splitting is 1.23 V (i.e., 2.46 eV/ $2e^-$) [23].

The water-splitting reaction comprises two half-reactions: water oxidation and water reduction.

$$2H^+ +\ 2e^-\ \rightarrow\ H_2\ (g)\ \ \text{(Water reduction)} \qquad (1.2)$$

$$2H_2O\ (l)\ \rightarrow\ 4H^+ +\ 4e^- +\ O_2\ (g)\ \ \text{(Water oxidation)} \qquad (1.3)$$

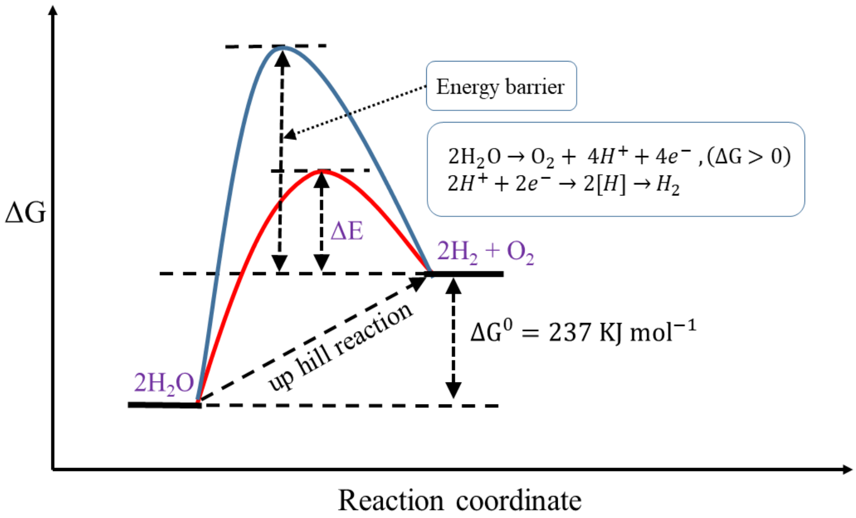

Fig. 1.5: Schematic of Gibbs free energy change in water splitting [25].

Water oxidation involves transferring four electrons to remove four protons and form an oxygen-oxygen bond. As a result, the splitting of water is driven by energy and can be fueled by solar energy (photocatalytic), electrical energy (electrochemical), or a combination of both (photoelectrochemical).

1.5.1 Solar water splitting

Using solar energy to directly split water into hydrogen and oxygen is highly promising and renewable [26]. This process requires semiconductors to efficiently absorb solar light with a minimum photon energy of 1.23 eV, equivalent to a wavelength of ~1000 nm, as shown in Figure 1.6(a). The semiconductor must generate at least two electron-hole pairs to produce one hydrogen molecule, requiring a minimum energy of 2.46 eV (2 x 1.23 eV). Figure 1.6(b) shows a self-sufficient device designed for a complete water-splitting reaction when exposed to solar light. The Nocera group has demonstrated that this device can split water into hydrogen and oxygen without external energy [27]. One component of the device is a Co-based catalyst deposited on ITO-coated Si, which facilitates the water oxidation OER in producing oxygen and generating protons. On the other side of the device, where the protons are reduced, the NiMoZn alloy acts as the catalyst for HER.

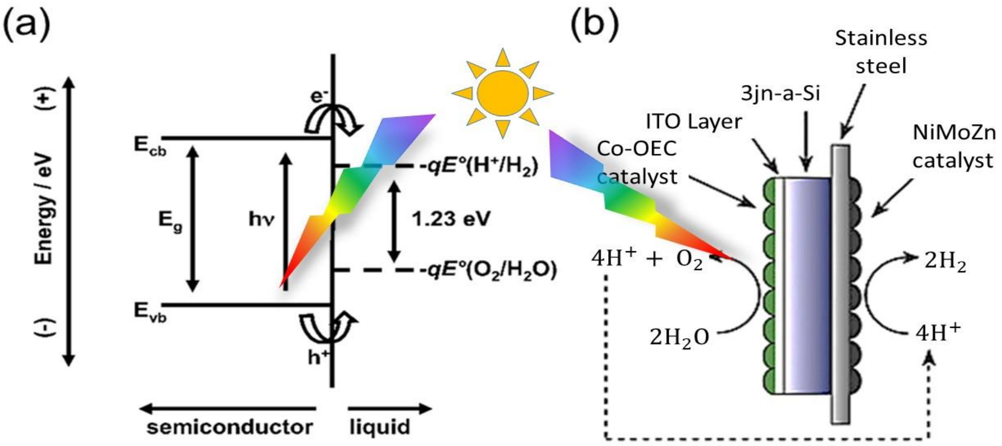

Fig. 1.6: Depicts the process of water splitting, showing (a) the half-cell reactions taking place on a semiconductor and (b) water splitting from a self-sustained solar device [27].

1.6 Fundamentals of water splitting

The O-H bonds in water are strong and need a lot of energy to be separated. The overall water-splitting reaction can be written as:

$$2H_2O\ (l) \rightarrow 2H_2 + O_2\ (g) \tag{1.4}$$

The hydrogen evolution reaction (HER) and the oxygen evolution reaction (OER) are two half-cell reactions.

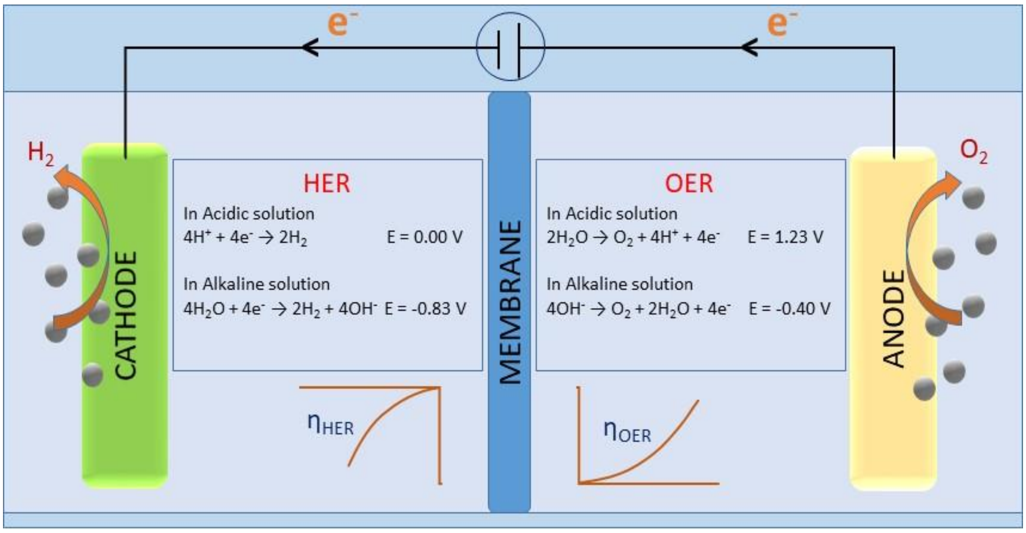

Fig. 1.7: Schematic representation of water splitting.

Reaction in acidic medium

HER: $2H^+ + 2e^- \rightarrow H_2\ (g)$

OER: $2H_2O\ (l) \rightarrow 4H^+ + 4e^- + O_2\ (g)$

Reaction in alkaline medium

HER: $2H_2O + 2e^- \rightarrow H_2\ (g) + 2OH^-$

OER: $4OH^- \rightarrow 2H_2O + 4e^- + O_2\ (g)$

The HER occurs at a standard potential of 0 V vs. a reversible hydrogen electrode (RHE), while the OER happens at 1.23 V versus RHE. This potential difference corresponds to a Gibbs free energy (ΔG) of 237.2 kJ/mol at 25°C. Consequently, despite the theoretical requirement of a 1.23 V potential for the reaction, practical applications often require much higher potentials, as explained in Equation 1.5.

$$E_{actual} = E^0 + \eta_a + \eta_c + iR \qquad (1.5)$$

where η_a and η_c denote the overpotentials at the anode and cathode, respectively, while i represent the current. The term "R" encompasses the resistance from various factors, such as bubble formation, inadequate electrical connections, and solution resistance. These challenges can be reduced by taking appropriate precautions and actions, such as inducing forced convection through rotation and optimizing the cell. Electrocatalysis functions based on the same principles as heterogeneous catalysis: the reactants diffuse to the catalyst surface, adsorb, undergo dissociation, and the resulting intermediates recombine through various mechanisms before the final product desorbs from the surface.

The catalyst's surface is where the HER takes place, distinct from the "outer sphere reaction" that happens over a layer of adsorbed electrolyte molecules. The material's characteristics largely influence the efficiency of the reaction. Although there isn't complete agreement on the precise mechanism of the hydrogen evolution reaction, the following two pathways are typically acknowledged (refer to Table 1.2 & Figure 1.8) [28].

The Volmer-Tafel pathway operates under the "Langmuir-Hinshelwood" mechanism. Initially, the reduction of a proton (H^+ in acidic conditions; H_2O in alkaline conditions) occurs, leading to the formation of an intermediate, H_{ad}, which then binds to the catalyst surface (Volmer step). Subsequently, another H_{ad} species combines with the first species, releasing an H_2 molecule (Tafel step).

The Volmer-Heyrovsky route follows the "Eley-Rideal" mechanism, where the initial step is similar to the Volmer-Tafel pathway. However, it differs by forming a heterolytic bond in the subsequent step.

Table 1.2 Hydrogen evolution reaction mechanism at different reaction steps.

Reaction step	Reactions	Electrolyte	Equation number
Volmer	$H^+ + e^- \rightarrow H_{ad}$ $H_2O + e^- \rightarrow H_{ad} + OH_{acid}$	Acid Base	1.6
Heyrovsky	$2H_{ad} \rightarrow H_2$	Acid/Base	1.7
Tafel	$H_{ad} + H^+ + e^- \rightarrow H_2$ $H_{ad} + H_2O + e^- \rightarrow OH^- + H_2$	Acid Base	1.8

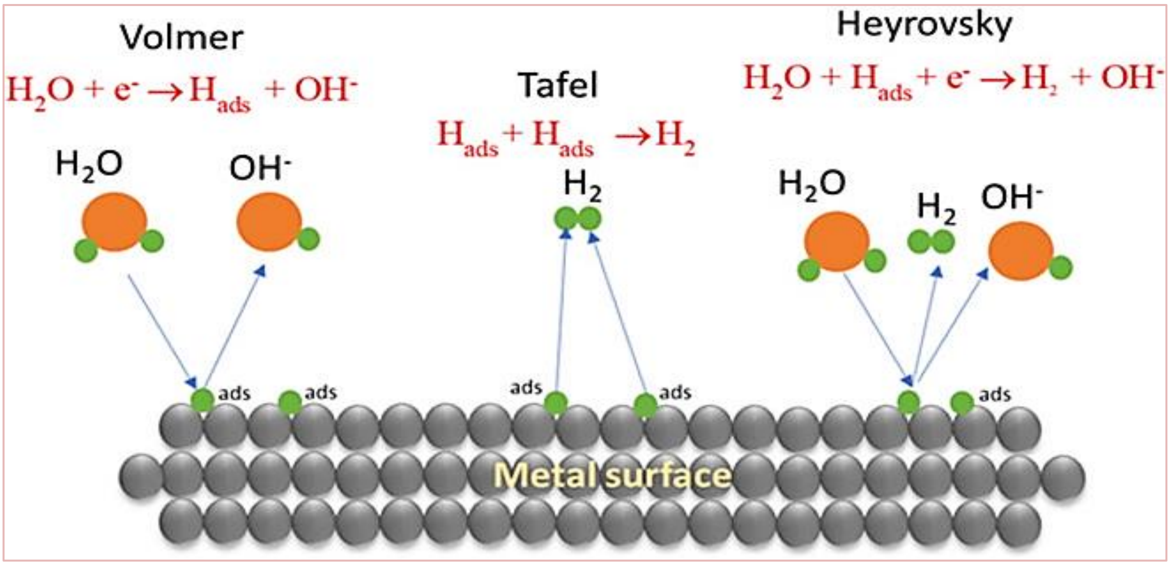

Fig. 1.8: Schematic representation of Volmer, Tafel, and Heyrovsky steps in alkaline HER [29].

Active materials catalyze HER and OER at minimal overpotentials while achieving high current densities to decrease the restriction stated by the reaction kinetics. The electrochemical kinetics are investigated using the Butler-Volmer equation (BVE). The BVE for a specific reaction consists of anodic and cathodic components, as illustrated in equation 1.8 [30].

$$\mathrm{I} = \mathrm{I}_0 \left[\exp \underbrace{(\alpha_a n\eta F/RT)}_{\text{Anodic}} - \exp\underbrace{(\alpha_c n\eta F/RT)}_{\text{Cathodic}}\right] \tag{1.9}$$

where n is the number of transferred electrons, I is the current density, I_0 represents the exchange current density, F represents Faraday's constant (96,485 C/mol), and $\eta = (E - E_{eq})$ is the overpotential, R is the universal gas constant, T is temperature, α_a and α_c are charge transfer coefficients for anodic and cathodic reactions, respectively. When the overpotential is very high, the influence of either the anodic or cathodic process diminishes substantially, resulting in the Butler-Volmer equation simplifying into the Tafel equation [31].

$$\mathrm{I}_a = \mathrm{I}_0 \exp\left(\frac{\eta}{b}\right) \tag{2.0}$$

$$I_c = I_0 \exp\left(\frac{\eta}{b}\right) \tag{2.1}$$

In the standard procedure, the log of current density (I_a for anodic and I_c for cathodic) is plotted as a function of overpotential. This produces two essential values: the Tafel slope (b) and the exchange current density (I_0). The (I_0) (in mA/cm²) value should be higher, and the Tafel slope should be lower (in mV/dec) for the best catalytic performance.

1.7 Photoelectrochemical hydrogen evolution reaction

In the photoelectrochemical (PEC) HER, protons (H^+) or water are reduced to form hydrogen molecules (H_2) under the influence of light. This reaction is driven by applying an external potential or electrochemical energy. This process involves a photoelectrode, usually composed of a semiconductor material, capturing photons from a light source and creating electron-hole pairs. Under the influence of the applied potential, the electrons move towards the cathode, where they reduce protons or water molecules to generate hydrogen gas. At the same time, the holes travel to the anode, where they participate in oxidation reactions. This technique utilizes light energy to improve hydrogen production efficiency, offering a sustainable method for producing clean fuel.

1.7.1 The overall reaction in HER

The HER reactions overall can be expressed as follows:

In acidic medium, $2H^+ + 2e^- \rightarrow H_2\,(g)$

In alkaline medium, $2H_2O + 2e^- \rightarrow H_2\,(g) + 2OH^-$

1.7.2 Mechanism involved in HER

The HER mechanism follows a two-step mechanism [32]: (i) the electrochemical adsorption, which is also known as the Volmer reaction, involves a proton (H^+) attaching to the metal catalyst's surface; (ii) electrochemical desorption, a process known as the Heyrovsky reaction, or through chemical desorption, referred to as the Tafel reaction.

Volmer reaction:

$$H^+ + e^- + M(\text{catalyst}) \rightleftharpoons MH_{ads} \text{ (acidic medium)}$$

$$\text{Or,} \quad H_2O + e^- + M\ (\text{catalyst}) \rightleftharpoons MH_{ads} + OH^- \text{ (alkaline medium)}$$

Heyrovsky reaction:

$$H^+ + e^- + MH_{ads} \rightleftharpoons M + H_2 \text{ (acidic medium)}$$

$$\text{Or,} \quad H_2O + e^- + MH_{ads} \rightleftharpoons M + OH^- + H_2 \text{ (acidic medium)}$$

And Tafel's reaction:

$$2MH_{ads} \rightleftharpoons 2M + H_2$$

Consequently, it can adhere to either the Volmer-Tafel or the Volmer-Heyrovsky mechanism.

1.7.3 Tafel slope in HER

The Tafel slope is crucial in exposing the HER process. If the discharge reaction is fast, and the chemical desorption (combination) is the rate-limiting step, then the Tafel slope is written as.

$$b = \frac{2.3RT}{2F} = 0.029\ \text{V/dec at } 25^0\text{C} \qquad (2.2)$$

A 29 mV/dec of Tafel slope is observed for Pt and Pd electrodes. When the Volmer reaction (discharge reaction) is fast, and the Heyrovsky reaction (electrochemical desorption) is the slowest step, then the Tafel slope is written as:

$$b = \frac{4.6RT}{3F} = 0.038\ \text{V/dec at } 25^{0}\text{C} \qquad (2.3)$$

When the Volmer reaction (discharge reaction) is the sluggish step, then the Tafel slope is written as:

$$b = \frac{4.6RT}{F} = 0.116\ \text{V/dec at } 25^{0}\text{C} \qquad (2.4)$$

A similar Tafel slope of 116 mV/dec is observed when the Volmer reaction is exceedingly fast, with the desorption step as the rate-determining step.

1.8 Evaluation parameters for PEC hydrogen production

The primary metrics for evaluating photoelectrochemical hydrogen production involve overpotential at specific current densities, Tafel slope, exchange current density, turnover frequency (TOF), faradaic efficiency and mass, and specific activities. The Tafel slope, exchange current density, and TOF provide insight into the reaction rate. Some critical factors to understand the PEC-HER performance are listed below:

1) **Overpotential**

   Overpotential (η) is the extra potential required to overcome the intrinsic kinetic barrier in PEC water-splitting for OER and HER [33]. In the process of HER and OER, the reversible thermodynamic potential is 0 and 1.23 V. The overpotential without iR compensation at a desired current density can be written as; $\eta_{HER} = E_{RHE} - 0$ V and $\eta_{OER} = E_{RHE} - 1.23$ V.

2) **Turnover frequency**

Turnover frequency (TOF) is a kinetic metric that measures the rate at which a photoelectrocatalyst facilitates the electrochemical reaction at a given overpotential. It is determined by counting the moles of O_2 or H_2 gas produced at every particular catalytic site. Both HER and OER follow pseudo-first-order kinetics, resulting in TOF in time. Mass loading does not impact TOF during the reaction but is significantly influenced by high coverage, with a linear relationship evident only if the coverage is less than 100% [34][35]. The higher the TOF value, the more influential the catalyst.

$$\mathrm{TOF} = \frac{\mathrm{j} \times \mathrm{N_A}}{\mathrm{n} \times \mathrm{F} \times \Gamma} \tag{2.5}$$

where the symbol j represents the current density (in A/cm^2), n denotes electrons transferred during the reaction process, N_A refers to Avogadro's number, F represents the Faraday constant, and Γ represents the total or surface concentration of active sites on the catalysts or the quantity of participating atoms in the photocatalyst material.

3) **Solar to hydrogen efficiency**

Solar to hydrogen efficiency (η_{STH}) is one of the most crucial factors in PEC hydrogen production. It estimates the hydrogen production efficiency through water splitting using solar solar light. It indicates the percentage of solar energy converted to the chemical energy stored in hydrogen. One of the most straightforward formulas for η_{STH}, assuming a Faradaic efficiency of 100%, is described as follows [36]:

$$\eta_{\mathrm{STH}} = \frac{\mathrm{j} \times 1.23\ (\mathrm{V})}{\mathrm{P_{in}}\ (\mathrm{W/m^2})} \tag{2.6}$$

where the symbol j indicates photocurrent density at 0 V bias, P_{in} indicates the input solar power.

4) **Stability**

The stability of a photoelectrocatalyst is a vital factor in its potential for large-scale commercial applications, as it assesses the catalyst's performance over extended periods. The catalyst's stability for HER and OER can be evaluated by cycling within the potential window using two methods: cyclic voltammetry (CV) or linear sweep voltammetry (LSV) at elevated scan rates, known as accelerated degradation tests and through extended potentiostatic or galvanostatic characterizations [37]. The number of cycles indicating the catalyst's stability differs for HER and OER. In HER, thousands of cycles are feasible as the polarization curve starts at 0 V vs. NHE. The shifts in onset potential and overpotential at a 10 mA/cm^{-2} current density are key indicators of photoelectrocatalyst performance. The catalyst is suitable if the overpotential increase is no more than 30 mV and the final activity degradation after stability testing is < 5%.

1.9 Issues in PEC cells

PEC cells have significant potential for sustainable hydrogen production and other uses. However, they encounter several challenges and constraints that must be resolved to enable their broad implementation. Some of the issues associated with PEC cells include low light absorption efficiency, low photocurrent density, low solar to hydrogen efficiency, charge carrier recombination, corrosion and oxidation, high-cost materials, electrolyte degradation, slow reaction kinetics, high overpotential, high tafel slope, and low turnover frequency. Among these problems, low photocurrent density, low turnover frequency, and low solar-to-hydrogen efficiency are the major problems in investigating the performance of PEC cells.

Several research studies are being conducted to find a solution to overcome the above problems. Li et al. [38] synthesized octahedral flower-like CuO nanocrystals through a coordination-deposition method and a modified Fehling reaction, which they found to be effective for large-scale synthesis. The researchers observed that adjusting the concentration of tartrate ions and the reaction duration has remarkably influenced the formation of the hierarchical nanostructures. These flower-like CuO nanocrystals, with a porous surface and a bandgap of 1.5 eV, demonstrated a peak photocurrent density of -58.8 $\mu A/cm^2$. Ray et al. [39] introduced a low-cost chemical bath deposition method to develop CuO photocathodes. In their work, they reported that the nanostructured CuO photocathodes were calcined at 200 °C and showed the highest photocurrent density of -1.3 mA/cm^2 due to enhanced photogeneration of electron-hole pairs across direct band edges with a suitable bandgap of 1.55 eV. To obtain high performance of CuO photocathode, Jang et al. [40] developed a hybrid microwave annealing (HMA) technique. They obtained an impressive photocurrent density of -4.4 mA/cm^2 for water splitting, possibly due to improved charge mobility and lower charge recombination rates owing to the structure's high purity and crystallinity.

Zhao et al. [41] conducted a different method to create a CuO/ZnO heterostructure. They fabricated CuO/ZnO core/shell NW arrays by thermally oxidizing copper foil to form cores. Subsequently, they applied a saturated ethanol solution containing zinc acetate onto the CuO NWs and subjected it to further thermal treatment at 350 °C for 20 minutes in the air. The resulting photoelectrode exhibited a 0.71% photon-to-hydrogen efficiency for PEC water splitting. Dubale et al. [42] developed a highly efficient Cu_2O/CuO photocathode with Ni decoration for water reduction using a simple, cost-effective method. The bare Cu_2O/CuO heterojunction fabricated at 450°C for 4 hours achieved the highest photocurrent density of -2.1 mA/cm^2 and 53% stability, owing to its improved crystalline quality and the synergistic effects of the CuO layer. Decorating the Cu_2O/CuO heterojunction with a Ni co-catalyst improved the photocurrent density to -4.3 mA/cm^2 at 0 V vs. RHE. The Ni-decorated photocathode maintained approximately 87.7% of the initial photocurrent density after 20 minutes of illumination, showing superior resistance to photocorrosion compared to the bare photocathode. It also reached a maximum solar conversion efficiency of 2.71% at an applied potential of -0.4 V.

The primary goal of all the above-reported works is to achieve high photocurrent density and improved photocatalytic performance for HER. The low photocurrent density may be due to charge carrier recombination, poor light absorption, and poor electrode stability. The high current densities at which industrial electrolyzers operate result in high ohmic losses directly proportional to the current. High electrolyte conductivities are necessary to reduce these losses, as predicted by Kohlrausch [43].

1.10 Materials for PEC cells

PEC cells show great potential for sustainable hydrogen production by harnessing solar energy to drive water-splitting reactions. Selecting suitable materials is crucial for maximizing the efficiency and durability of PEC cells. Semiconductors such as TiO_2 [44], ZnO [45], $BiVO_4$ [46], and CuO [47], etc. are commonly used as photocathodes due to their ability to absorb sunlight, stability in water and effectiveness in catalyzing the hydrogen evolution reaction (HER). Incorporating co-catalysts like platinum or nickel-based compounds can significantly boost the overall efficiency of PEC cells by reducing overpotentials and accelerating reaction rates.

In the last few decades, there has been a surge in interest in solar hydrogen production. In 1998, Khaselev and Turner [48] introduced p-GaInP2(Pt)/TJ/GaAs electrode as a photoelectrochemical (PEC) water-splitting system that integrated solar energy harvesting and water electrolysis into a single device, achieving a solar-to-hydrogen (STH) conversion efficiency of 12.4%. Some of the most promising, cost-effective, and efficient materials for PEC cells are:

1.101 Titanium Dioxide (TiO_2) – TiO_2-based photoelectrodes have been extensively researched for water splitting since 1972, owing to their favorable properties, including the use of earth-abundant and non-toxic materials, and their high photochemical stability in basic and acidic conditions [49]. Nonetheless, TiO_2's wide band gap (3.2 eV for anatase and 3.0 eV for rutile) limits its ability to absorb only about 5% of the solar spectrum, primarily in the UV range, which results in a low theoretical maximum STH efficiency (~ 1.3% for anatase and 2.2% for rutile). Li, Shipu, and colleagues [50] developed Si nanowire (SiNW) arrays coated with Pt nanoparticles and fully passivated with an amorphous TiO_2 layer using atomic layer deposition (ALD), which demonstrates superior PEC performance compared to other photoelectrodes, particularly in terms of chemical stability and photoresponse under both standard 1 sun and concentrated light conditions. The TiO_2/Pt/SiNW photoelectrode achieves a peak cathodic photocurrent of approximately -27 mA/cm^2 under 100 mW/cm^2 illumination, increasing to -65 mA/cm^2 under 300 mW/cm^2 illumination. The onset potential for the TiO_2/Pt/SiNW sample is 0.35 V versus RHE. In the past decade, significant efforts have been directed toward doping TiO_2 with various anions or cations to extend its absorption into the visible light range and enhance overall absorption while maintaining stability. The valence band can be altered by incorporating non-metal elements like carbon or nitrogen, which introduce mid-gap states [51], and its conduction band can be adjusted by doping with 3d transition metal ions, forming donor states below it. However, these approaches typically do not alter the fundamental band gap, and as a result, no significant enhancement in visible-light-driven PEC water-splitting efficiency has been observed.

1.102 Bismuth Vanadate ($BiVO_4$) – Bismuth vanadate (BVO), an n-type semiconductor composed of relatively plentiful elements, has a direct band-gap of 2.4 eV, with its conduction band near 0 V vs. NHE (pH = 0) and its valence band at about +2.4 V vs. NHE (pH = 0). Initially discovered by Kudo et al. [52] for photocatalytic water oxidation in the presence of sacrificial agents, BVO has since also been employed as a photoanode in PEC water splitting, with progress in this area extensively reviewed in other sources [53]. BVO can theoretically achieve a maximum photocurrent density of ~ 7.4 mA cm^{-2} at 1.23 V vs. RHE and an STH efficiency of ~ 9.1%. Despite this, rapid charge carrier recombination limits its efficiency, which is linked to its short electron diffusion length of about 10 nm and inadequate kinetics for water oxidation at the surface.

1.103 Cuprous Oxide (Cu_2O) – Cuprous oxide features a direct band gap of ~ 2 eV, with a conduction band position at approximately -1.1 eV vs. NHE, which makes it well-suited for light-induced hydrogen generation from water. Cu_2O is very attractive due to its abundance, ease of scaling, low toxicity, high theoretical photocurrent of roughly 15 mA cm^{-2}, and expected STH efficiency of 18% under AM 1.5G solar illumination, as reported by Cheng, J. et al. [54]. Cu_2O faces the challenge of a relatively moderate photocurrent attributed to fast electron-hole recombination. Additionally, its poor stability poses a significant drawback, as the redox potentials that reduce and oxidise the monovalent copper oxide are situated within the band gap.

1.104 Graphitic Carbon Nitride (g-C_3N_4) – Graphitic carbon nitride, having band gap energy of ~ 2.7 eV and consisting of carbon (C) and nitrogen (N), is considered one of the leading metal-free photocatalysts [55][56]. Its popularity stems from its ease of production, customizable electronic properties, remarkable physical and chemical attributes, and impressive electronic behavior across various applications. To address this challenge, a growing interest is in utilizing g-C_3N_4 within composite compounds. In a study by Hosseini H. et al. [57], the effects of composing g-C_3N_4 with CuO and subjecting the nanocomposite electrode to heat treatment on PEC performance were examined. The researchers synthesized CuO micro-flowers made up of interlinked ultrathin nanosheets and hierarchical carbon-doped CuO dandelions/g-C_3N_4 (C–CuO/CN) nanocomposites. The synthesis process involved using copper sulfate and urea in an alkaline environment through one-pot microwave irradiation. The report indicated that the C–CuO/CN photoelectrode achieved a maximum photocurrent density of -2.85 mA cm^{-2} at 0 V versus RHE under AM 1.5G light. The highest rate of hydrogen evolution for the C–CuO/CN nanocomposite was around 3.13 μmol h^{-1} cm^{-2}. However, pure g-C_3N_4 suffers from significant electron-hole recombination, which hampers its efficiency.

1.105 Molybdenum Sulphide (MoS_2) – Molybdenum sulfides, having a band gap of ~ 1.9 eV, have been the center of extensive research in recent years as co-catalysts for PEC hydrogen production. Zong et al. [58] reported MoS_2 as a co-catalyst for the first time by forming a MoS_2/CdS heterojunction, which was applied to photocatalytic hydrogen production. They observed the rate of hydrogen evolution of the MoS_2/CdS system was higher than that of the Pt/CdS system. The p-n heterojunction formed between MoS_2 and CdS significantly enhances the transfer of photogenerated carriers, thereby boosting the photocatalytic activity. In this context, MoS_2 serves as a non-noble metal co-catalyst, offering an alternative to precious metals. Morales-Guio et al. [59] achieved successful photoelectrochemical (PEC) hydrogen evolution by combining an amorphous MoS_x electrocatalyst with copper (I) oxide (Cu_2O). They enhanced photovoltage by incorporating a 20 nm layer of aluminum-doped zinc oxide (AZO) to form a buried Cu_2O/AZO photovoltaic junction. Additionally, a 100 nm titanium dioxide (TiO2) film was deposited using atomic layer deposition to shield the junction from the aqueous environment and aid in the transfer of photoinduced electrons to the electrolyte for water reduction. The system achieved an onset potential of 0.45 V vs. RHE and a photocurrent density of up to 5.7 mA/cm^2 at 0 V vs. RHE (pH 1.0) under simulated AM 1.5 solar illumination.

1.106 Copper Oxide (CuO) – CuO stands out as a few photocatalysts that show high effectiveness in PEC hydrogen evolution reaction (HER) under simulated solar light, especially in conjunction with other photocatalysts [60]. Theoretical studies indicate that CuO-based photocathodes have the potential to achieve a peak photocurrent density of 35 mA cm^{-2} [61]. Mahmood et al. investigated the impact of electrodeposition time on the photoelectrochemical (PEC) properties and microstructure of CuO films. In their study, CuO films were deposited on ITO substrates with varying deposition times ranging from 300 to 1800 seconds, followed by a heat treatment at 550 °C for 2 hours. The maximum photocurrent density they obtained was 0.55 mA/cm^2 at 0.5 V [62].

Besides the good performances shown by the above-listed materials, there are some cons that hinder the overall performance of PEC cells, which need to be tackled to achieve the maximum performance of PEC cells. Some of the challenges that need to be focused on are high photocurrent density, reduced recombination loss, using dopants with better light absorption properties, and a strategy to prevent the photocathode from corrosion. Our work mainly focuses on utilizing cost-effective photocathodes with the best PEC performance. These include achieving high HER photocurrent density, increasing solar to hydrogen efficiency, reducing corrosion current density, and fast charge carrier dynamics. In order to accomplish this, we have fabricated self-assembled CuO/Cu_2O ultrathin films and obtained high solar to hydrogen efficiency of ~12.2%. Here, nanostructuring plays a vital role in enhancing the PEC performance. So, we have synthesized CuO nanoparticles to check the photocurrent stability and achieved a high photocurrent density of -41.57 mA/cm^2 at 0.6 V vs. RHE, and also the chronoamperometric results indicated that the photocurrent density was stable for 4000 seconds. Further, we synthesized a $\mathrm{Cu_{1-x}Ni_xO}$ $(x = 0, 0.2, 0.4, 0.6, 0.8, 1)$ system by doping NiO in CuO in the stoichiometric ratio and from the HER result, a remarkable photocurrent density of -42.64 mA/cm^2 at 0 V vs RHE was observed.

1.11 The objective of current research

The main objective of current research work is to explore and use cost-effective CuO-based photocathodes to improve photoelectrochemical performance for enhanced hydrogen production. CuO is one of the promising materials that has shown its potential to replace expensive catalysts such as Platinum (Pt) for PEC H_2 production. The primary focus involves improving photocurrent density, increasing solar-to-hydrogen (STH) efficiency, and maximizing hydrogen production.

Some of the points that are focused in this research work to improve the photoelectrochemical cell performance are:

a) Increasing HER photocurrent density.
b) Enhancing solar to hydrogen efficiency.

c) Enhancing hydrogen production.

For this purpose, CuO nanoparticles, CuO/Cu_2O thin films, and $Cu_{1-x}Ni_xO$ systems were selected as potential photocathode materials for PEC hydrogen production. Further, a detailed information of the synthesis process and measurement techniques for the compounds investigated are described in the next chapter.